Plate-boundary deformation associated with the great Sumatra–Andaman earthquake

Subarya, Cecep; Chlieh, Mohamed; Prawirodirdjo, Linette; Avouac, Jean-Philippe; Bock, Yehuda; Sieh, Kerry; Meltzner, Aron J.; Natawidjaja, Danny H.; McCaffrey, Robert

2006

Subarya, C., Chlieh, M., Prawirodirdjo, L., Avouac, J. P., Bock, Y., Sieh, K., et al. (2006). Plate-boundary deformation associated with the great Sumatra–Andaman earthquake. Nature, 440, 46-51.

https://hdl.handle.net/10356/94250

https://doi.org/10.1038/nature04522

Plate-boundary deformation associated with the great Sumatra–Andaman earthquake

Cecep Subarya[1], Mohamed Chlieh[2], Linette Prawirodirdjo[3], Jean-Philippe Avouac[2], Yehuda Bock[3], Kerry Sieh[2], Aron J. Meltzner[2], Danny H. Natawidjaja[4] & Robert McCaffrey[5]

[1]National Coordinating Agency for Surveys and Mapping, Cibinong 16911, Indonesia.

[2]Tectonics Observatory, Division of Geological and Planetary Sciences, California Institute of Technology, Pasadena, California 91125, USA.

[3]Cecil H. and Ida M. Green Institute of Geophysics and Planetary Physics, Scripps Institution of Oceanography, University of California San Diego, La Jolla, California 92093, USA.

[4]Research Center for Geotechnology, Indonesian Institute of Sciences, Bandung 40135, Indonesia.

[5]Department of Earth and Environmental Sciences, Rensselaer Polytechnic Institute, Troy, New York 12180, USA.

Correspondence and requests for materials should be addressed to J.-P.A. (avouac@gps.caltech.edu).

The Sumatra–Andaman earthquake of 26 December 2004 is the first giant earthquake (moment magnitude M_w > 9.0) to have occurred since the advent of modern space-based geodesy and broadband seismology. It therefore provides an unprecedented opportunity to investigate the characteristics of one of these enormous and rare events. Here we report estimates of the ground displacement associated with this event, using near-field Global Positioning System (GPS) surveys in northwestern Sumatra combined with *in situ* and remote observations of the vertical motion of coral reefs. These data show that the earthquake was generated by rupture of the Sunda subduction megathrust over a distance of >

1,500 kilometres and a width of < 150 kilometres. Megathrust slip exceeded 20 metres offshore northern Sumatra, mostly at depths shallower than 30 kilometres. Comparison of the geodetically and seismically inferred slip distribution indicates that ~30 per cent additional fault slip accrued in the 1.5 months following the 500-second-long seismic rupture. Both seismic and aseismic slip before our re-occupation of GPS sites occurred on the shallow portion of the megathrust, where the large Aceh tsunami originated. Slip tapers off abruptly along strike beneath Simeulue Island at the southeastern edge of the rupture, where the earthquake nucleated and where an M_w = 7.2 earthquake occurred in late 2002. This edge also abuts the northern limit of slip in the 28 March 2005 M_w = 8.7 Nias–Simeulue earthquake.

The great Sumatra–Andaman earthquake of 2004 was produced by rupture of the Sunda subduction megathrust, along which the Indian and Australian plates subduct northeastward beneath the Sunda shelf (Fig. 1). Southeast of Sumatra, at Java, convergence is nearly orthogonal to the plate boundary at ~63–68 mm yr^{-1} (refs 1, 2). Along Sumatra the convergence is oblique to the trench and the relative plate motion is partitioned into nearly perpendicular thrusting on the megathrust at ~45 mm yr^{-1} and trench-parallel, right-lateral slip along the Sumatra fault at ~11 to 28 mm yr^{-1} (refs 3, 4). The convergence rate normal to the trench is ~40 mm yr^{-1} near the 2004 epicentre off northern Sumatra and decreases northwards as the megathrust strike becomes nearly parallel to the direction of relative plate motion. North of 8° N, sparse geodetic data suggest a convergence rate normal to the trench of between 14 and 34 mm yr^{-1} (refs 5, 6).

The Sumatran section of the Sunda megathrust generated great earthquakes south of the 2004 event in 1797, 1833 and 1861 (refs 7–9) but there is no historical record of giant earthquakes to the north, between Sumatra and Myanmar (Fig. 1).

Analyses of high-frequency seismic records of the December 2004 earthquake obtained from the Global Seismic Network[10], from an array of seismic stations in Thailand[11] and from T-waves recorded in the Indian Ocean[11,12], indicate that the rupture took about 500 s

to propagate a straight-line distance of ~1,300 km from the hypocentre in northern Sumatra to the northern Andaman Islands. This rupture area roughly coincides with the distribution of aftershocks[6,11] (Fig. 1). A model of the slip history and its spatial distribution obtained by combining body waves and surface waves yielded a total seismic moment for the earthquake of 6.5×10^{22} N m, released mostly between latitudes 2° N and 10° N, corresponding to $M_w = 9.1$ (refs 13, 14).

We report here on near-field GPS observations of deformation and *in situ* and remotely sensed observations of uplift and subsidence of coral reefs. We use these to constrain the distribution of slip on the Sunda megathrust during and soon after the 26 December 2004 earthquake, and to compare it to slip models derived from seismic data. These geodetic data allow us to model in great detail the slip distribution west of northern Sumatra, the region of greatest devastation.

GPS measurements

Our re-survey of GPS monuments in northern Sumatra between 28 January and 19 February 2005 reveals combined coseismic and postseismic displacements of up to several metres associated with the earthquake (Fig. 2). One set of monuments was surveyed three or four times in the years 1991–2001 (refs 15 and 16) and provides a record of pre-earthquake interseismic velocities[1]. This GPS network includes lines of closely spaced points across the Sumatran fault[4], including one in northernmost Aceh, across the region of greatest devastation from the ensuing tsunami. A second set of monuments was surveyed only once before the earthquake by the Indonesian National Coordinating Agency for Surveys and Mapping (BAKOSURTANAL) as part of geodetic control for Sumatra. One of these sites (R171) is on Selaut Besar, a small island north of Simeulue Island, only about 50 km from the earthquake's epicentre (Fig. 3a). We used the decade-long pre-earthquake GPS measurements to construct a kinematic model of interseismic deformation that allowed us to correct the measured displacements for steady inter-seismic motions (Table 2 in Supplementary Information 1).

Continuous GPS data from BAKOSURTANAL's site SAMP (Fig. 3a) reveal a clear record of coseismic and postseismic deformation. The daily time series shows a

coseismic horizontal displacement of 138mm that increased logarithmically with time after the main shock by ~15% over 15 days, and ~25% over 30 days. For comparison continuous measurements at site PHKTon the island of Phuket indicate a coseismic slip of 270 mm, which increased by ~22% over 30 days (ref. 17). Although these two records reveal significant post-earthquake motion, they do not show how widespread or variable it was. Continuous GPS data from the Sumatran GPS Array (SuGAr; http://www.tectonics.caltech.edu/sumatra/data.html), more than 300 km south of the epicentre, show coseismic displacements typically less than 10mm and no detectable post-seismic transients.

We processed the raw survey-mode and continuous GPS data with the GAMIT/GLOBK software (http://www-gpsg.mit.edu/~simon/gtgk/)[18]. The data were analysed in 24-h segments (0–24 h GMT) with data from ten additional continuous GPS sites on Java, the Cocos Islands, Diego Garcia, Singapore, India, Australia and Guam. These solutions were combined with global GPS network solutions produced routinely at the Scripps Orbit and Permanent Array Center (http://sopac.ucsd.edu) to determine the GPS velocities and displacements and their uncertainties with respect to the ITRF2000 reference frame[19].

Uplift determined from field measurement of coral heads

At the southern end of the rupture, coral heads enabled measurement of uplift. We used their 'micro-atoll' morphology to measure pre-and post-earthquake sea level[9,20,21]. We measured these sea level proxies on 17 and 18 January and on 5 February 2005 at ten locations around Simeulue Island. We found the pre-quake highest level of survival to be systematically 0.2 to 1.5 m higher than the post-quake level, with values rising towards the northwest (Fig. 2 and Supplementary Information 1). Differences in low tide levels before and after the earthquake, computed according to an ocean-tide model[22], lead to adjustments of just a few centimetres[23]. The accuracy of the measurements, about ±50 to 100 mm, is only ~2–3 times worse than the vertical accuracy of typical field GPS geodetic measurements. The advantage of the coral measurements is that they form a dense array of points that constrains the tilting of Simeulue and therefore the gradient in

slip at the southern end of the underlying megathrust. We also collected less quantitative evidence of submergence around the southern half of Simeulue Island; at two localities these are eyewitness accounts of sea level changes. At another place we measured the depth of flooding of a well-drained locality where residents said water had never stood before.

Determination of uplift and subsidence from remote sensing

We used satellite imagery (ASTER, SPOT, IKONOS, QUICKBIRD and LANDSAT) to assess changes in relative sea level associated with the earthquake[23]. Because the colour and brightness of a reef in an image depend on water depth above the reef, changes in water depths of several centimetres or more are recognizable on the images. We examined satellite images of the Andaman and Nicobar islands and northwestern Sumatra to identify areas where reef or land exposure changed following the earthquake.

Satellite images acquired before 26 December 2004 were compared with images acquired between 26 December 2004 and 28 March 2005. We used a tidal model[22] (1-σ uncertainty of ~5 cm) to determine the relative sea surface height at each location at the acquisition time of each image. To document the uplift of a reef, we looked for a post-earthquake image with more reef exposure than a pre-earthquake image of the same area taken at a lower tide; in that case, the difference in sea surface height between the two images provides a minimum amount of uplift. Similarly, a pre-earthquake image with more exposure than a post-earthquake image at a lower tide indicates subsidence; in this case, the difference in sea surface height gives the minimum subsidence.

Although we can provide both maximum and minimum constraints on uplift or subsidence in a few locations, in most cases this method is limited by the tidal range; where uplift or subsidence exceeded the tidal range, we can provide only a minimum bound on the amount of tectonic elevation change. Nonetheless, the extrema of vertical displacements and the sign of the elevation change at a location are robust. Altogether we made such observations at 156 locations (Fig. 2). These data show detectable uplift from Simeulue to Preparis Island (Myanmar) over a distance of 1,600 km along the trench[23].

Fault slip distribution from inversion of geodetic data

Vertical ground displacements determined from the various techniques show a characteristic pattern: a region of uplift nearer the trench and a region of subsidence away from it (Fig. 2). The pivot line, which separates the areas of coseismic uplift and subsidence, approximates the easternmost extent of slip on the fault surface below. Where constrained by both uplift and subsidence observations, the pivot line of the 2004 earthquake lies between 80 and 120 km from the trench. In the area of the Nicobar Islands, all of which subsided, the pivot line is close to the westernmost islands[23], less than 150km from the trench. Observations of both uplift on northwestern Simeulue Island and subsidence on the southernmost part of the island also indicate that the southern, lateral limit of slip is beneath the island. These simple observations imply that the rupture area was confined to the shallow part of the subduction zone within about 150 km of the trench and did not extend south of Simeulue Island.

We estimate the three-dimensional distribution of slip on the megathrust by inverting the geodetic observations described above, GPS measurements from the Nicobar and Andaman islands (http://www.seires.net/content/view/123/52/, CESS website)[24], and continuous GPS offsets in Phuket and Medan (Fig. 3a, b). Because the uplift and survey-mode GPS observations were made a month or so after the earthquake, they probably contain displacements due to aftershocks and postseismic slip. Displacements directly associated with aftershocks are, however, relatively minor, because the total seismic moment from aftershocks is less than one per cent of that of the mainshock. We followed a two-step procedure in the inversion of the geodetic data (details in the Supplementary Information). To facilitate direct comparison of seismic and geodetic slip models, we first inverted the geodetic data using the same simplified fault geometry: three planar faults, and layered structure as in previous seismological models[14] (model A, Fig. 3a). Then, to assess the sensitivity of the results to the fault geometry and seismic velocity structure, we used a more realistic three-dimensional fault geometry, in a homogeneous half-space (model B, Fig. 3b). Details on these two models are given in the Supplementary Information.

In model A, the fault is represented by three overlapping planar segments with different strikes, and dip angles increasing from 12° in the south to 17.5° in the north, with the slab extending to about 125 km depth. In this model, our best estimate of the geodetic moment is 8.8×10^{22} N m, corresponding to a magnitude of $M_w = 9.22$. The weighted root-mean-square is 1.8 cm, corresponding to a reduced x^2 of 2.44. Sensitivity and resolution tests suggest that the model probably provides a lower bound on the estimated moment required to fit the geodetic data. The scalar seismic moment for the best-fit geodetic model is ~30% greater than the seismological estimate (Fig. 4). The geodetic model predicts remarkably well the azimuths of coseismic displacements observed at continuous GPS stations in Thailand and Malaysia[17] (Fig. 3a), but the amplitudes are systematically larger by an average of 26%. The seismological model[14] predicts displacements which also agree well with these azimuths, but underpredicts the amplitudes. When only the coseismic data (representing geodetic displacements over one day) from Thailand and Malaysia and at Medan are inverted, the geodetic moment is constrained to about 6.8×10^{22} Nm (as also estimated by Vigny *et al.*[17]), which is close to the seismic estimate. We conclude that the excess moment of the geodetic model over the seismic model, equivalent to about a $M_w = 8.7$ earthquake, reflects aseismic afterslip in the weeks following the earthquake, rather than slow aseismic slip during the first day after the earthquake, as proposed in some early studies[6,13].

In model B, the slip distribution is represented as three-parameter gaussian functions of depth along 26 trench-normal profiles between 1° N and 16° N. In cross-section, the modelled fault geometry, based largely on earthquake distributions, is curved downward and is on average steeper in the northern profiles. The 78 free parameters are estimated by least-squares fit to the 287 weighted observations, giving a reduced x^2 of 0.83, indicating the observations are matched closely at their levels of uncertainty. It also yields a seismic moment of $M_w = 9.22$ and slip that varies markedly along strike. Both models show three distinct patches of high slip from 4 ° to 6 ° N, 8 ° to 10 ° N, and 12 ° to 13.75 ° N. These patches probably correspond to the three distinct bursts of energy seen in the seismological inversions and attributed to patches of high slip[14]. Both models suggest a minimum rupture length of about 1,400 km, based on the area within which slip

exceeded 5 m. Given the uplift documented at Preparis Island[23] the rupture must have been somewhat longer: about 1,600 km. Both models display a prominent trough in slip values from about 7 ° to 8 ° N, which may reflect a lack of local geodetic measurements. Slip near the epicentre was relatively low (< 15 m) but ramped up dramatically northward to > 20 m. Model A places all slip at depths shallower than 50km. The more realistic curved geometry of model B yields a shallower slip distribution in which most slip was shallower than 25km depth. This shallowness of slip is the principal reason that the rupture generated the great tsunami.

Discussion

The 2004 Sumatra–Andaman earthquake illuminates the rupture processes of giant earthquakes. Such earthquakes are so rare that we have relied largely on empirical correlations between properties of megathrust earthquakes and their subduction zones to understand them. One widely accepted relationship[25,26] is that maximum earthquake magnitude on a given thrust increases linearly with convergence rate and decreases linearly with subducting plate age. The relatively small Car Nicobar and Andaman earthquakes of 1881 and 1941 (ref. 6), enveloped within the northern part of the 2004 rupture, fitted this pattern—the subducting lithosphere is old and converging at a moderate rate (Fig. 1). Backarc extension, like that east of the northern part of the 2004 rupture, has also been associated with low-magnitude maximum magnitudes[27,28]. The size of the 2004 earthquake is clearly at odds with these concepts. Thus, these empirical relationships must neglect important physical processes governing the seismicity of subduction zones. An alternative explanation for the distribution of large earthquakes at subduction zones over the past century is that these correlations result from a sample period that is too short—faster slipping subduction zones will on average produce larger earthquakes in a given time period because the repeat time of an earthquake of a given size is inversely related to the fault slip rate[29]. Perhaps we must now consider the possibility that, given a suitable length of time, any megathrust fault can produce an earthquake whose size is limited only by the available area of the locked fault plane. From 0.5° to about 6° S, the Sunda megathrust has produced two giant earthquakes in recorded history[7,30], and geodetic measurements show it has been fully locked above a

depth of 40 to 55 km for at least the past 50 years[1,31]. Further south, the long section of the Sunda megathrust adjacent to the densely populated island of Java subducts very old lithosphere and should, according to previous wisdom, not produce great quakes. The degree of locking of the megathrust and possibility of great earthquakes there should now be investigated.

Could we have forecast the width of the 2004 megathrust rupture? Analyses of the geodetic and paleogeodetic records of interseismic deformation a few hundred kilometres south of the epicentre suggest that the depth of the downdip end of the locked zone varies from ~30 to 55 km (refs 15, 31–33). No published geodetic or paleogeodetic data were available to constrain interseismic deformation in the area of the 2004 rupture. However, background seismicity provided a clue. Along intracontinental megathrusts, background seismicity tends to cluster around the downdip end of the locked fault zone[34]. Before December 2004, seismicity was clustered near the downdip end of the future rupture zone, at depths between 40 and 50 km (Fig. 3a). This suggests that the rupture remained confined to the shallow portion of the fault zone that was locked before the great event. Our results thus support the use of background seismicity as one indicator of the down-dip limits of future seismic ruptures.

Substantial afterslip followed the 2004 coseismic rupture. The geodetic data suggest that slip, equivalent to an M_w = 8.7 earthquake, occurred along the plate interface in the month following the 2004 earthquake. Afterslip downdip of the coseismic rupture is not uncommon[35–38], but the data do not reveal significant deep slip. The correlation between the zone with high slip determined from geodesy and the area that generated high-frequency body waves[14] suggests that early afterslip occurred on or close to the fault patch that underwent coseismic slip. It is possible that a significant fraction of afterslip occurred updip of the seismically ruptured area. However, the details of the spatial and temporal evolution of slip on the shallow plate interface during and after the event cannot be constrained because of the lack of data close to the trench.

The great horizontal extent of the rupture, which ultimately led to the great magnitude, would have been far more difficult to forecast. The along-strike variability of the

coseismic slip distribution (Fig. 3) might reflect past earthquake history, with areas of low slip corresponding to patches that ruptured during past events, or could indicate that the megathrust fault plane is a mix of aseismically slipping areas characterized by a rate-strengthening friction law, and areas of stick-slip behaviour, characterized by a rate-weakening friction law. The latter hypothesis is more plausible, given the correlation of historical $M_w > 7$ earthquakes with high-slip patches of 2004. The frictional and seismic properties of fault zones are thought to depend on a number of factors, including lithology, temperature, pore pressure and normal stress[39], that could act jointly to produce variable behaviour. Because aseismic creep is thermally activated, temperature might limit the bottom of the locked fault zone by promoting aseismic slip at depth[40]. Another possibility is that the downdip end of the locked fault zone coincides with the intersection of the plate interface and the forearc Moho, because stable sliding slip could occur along the serpentinized mantle wedge[40]. In the Sumatra–Andaman case, we discount this possibility because the forearc Moho intersects the megathrust well updip of the bottom of the interseismic locked zone[33]. To assess whether or not temperature might control the downdip extent of the ruptured area, we estimate the along-strike depth of the 350°C isotherm, a commonly assumed temperature at the downdip end of the locked section of subduction megathrusts. For an average shear stress between 20 to 40 MPa on the fault and for the variety of subduction dip-angles, this depth is around 40km in the epicentral area and does not vary much along strike from northern Sumatra to the northern Andaman Islands. This near-constancy in fault zone temperature occurs because the lower heat flow at the top of the older lithosphere in the north has longer to transmit heat to the upper plate owing to the lower trench-normal slip rate.

Still, temperature cannot easily explain short-wavelength lateral variations of frictional properties; other factors must control changes in behaviour. The high proportion of aseismic slip on the 2004 rupture plane may, for example, be due to a lubricating or pore-pressure effect of sediments from the Bengal fan subducting down along the megathrust. The thickness of the sediment reaching the trench is indeed great along the entire rupture, decreasing gradually southwards from more than 4 km to about 1 km (Fig. 1).

The large proportion of afterslip on the 2004 rupture and the irregular coseismic slip

pattern might indicate that much of the megathrust slips aseismically. If the proportion of aseismic to seismic slip during the 2004 Sumatra–Andaman earthquake is representative of the long-term average, aseismic slip might be of the order of 0.5 or greater in the Andaman and Nicobar area. The large fraction of aseismic slip may account for the common observation that seismic moment release along subduction zones falls short of the value estimated from the long-term slip rate along the seismogenic portion of the plate interface[41,42].

We estimate a nominal repeat time for the 2004 event by dividing the quake's potency (slip times rupture area; $1.7 \pm 0.1 \times 10^{12}$ m^3) by the long-term potency rate ($3–7 \times 10^9$ m^3 yr^{-1}), estimated from the area of the subduction interface north of 2° N (about 2.0×10^5 km^2), and the long-term average slip rate (24 ± 10 mm yr^{-1}). If all this slip was released only by the repetition of events like the Sumatra– Andaman earthquake, such events would occur on average every 230–600 years; if half of the slip is aseismic, or taken up by smaller events such as the events in 1881 or 1941, the recurrence time would double. Such long average return periods are consistent with no historical record of prior events.

A striking feature of the slip distributions we derived is the abrupt southern termination, required by the rapid southward decrease in coral uplift. Our measurements show that the southern limit of uplift in 2004 is approximately coincident with the northern limit of uplift during the 28 March 2005, M_w = 8.7 Nias–Simeulue earthquake (http://www.gps.caltech.edu/~jichen/Earthquake/2005/sumatra/preliminary/sumatra.html). The proximity of the 2004 and 2005 uplift terminations and a M_w = 7.2 foreshock on 2 November 2002 could reflect the presence of a structural feature that is an impediment to rupture propagation. Perhaps the long north-trending fracture zone on the seafloor of the Indian plate that projects to this point[7] has created a structural or rheological complexity in the megathrust beneath central Simeulue Island. Similar structural discontinuities on the sea floor may have influenced the termination points of large megathrust ruptures in 1861, 1833 and 1935 (refs 7,20), but the exact mechanism by which they might have done so remains elusive.

Acknowledgements

We thank the team from BAKOSURTANAL who collected the GPS field data in Sumatra under difficult conditions (J. Efendi, A. Indrajit, M. Nyamadi, C. Bagandi, D. Sudharmono, A. Suryono, M. Achmad, U. Santoso, C. Yuniarsa, Endang, A. Pujobuntoro, H. Dradjat, B. Susilo and B. Parjanto). We are grateful to C. Vigny for comments and suggestions. This work has benefited from discussions with C. Ji. The Gordon and Betty Moore Foundation, the US National Science Foundation, the Southern California Earthquake Center, and BAKOSURTANAL supported this research. We thank R. W. Matindas and J. McRaney for their support. This is Caltech Tectonics Observatory contribution number 31.

References

1. Bock, Y. *et al*. Crustal motion in Indonesia from Global Positioning System measurements. *J. Geophys. Res.* **108**(B8), 2367, doi:10.1029/2001JB000324 (2003).

2. Michel, G. *et al*. Crustal motion and block behaviour in SE-Asia from GPS measurements. *Earth Phys. Sci. Lett.* **187**, 239–244 (2001).

3. Sieh, K. & Natawidjaja, D. Neotectonics of the Sumatran fault, Indonesia. *J. Geophys. Res.* **105**, 28295–28326 (2000).

4. Genrich, J. F. *et al*. Distribution of slip at the northern Sumatran fault system. *J. Geophys. Res.* **105**, 722–743 (2000).

5. Paul, J. *et al*. The motion and active deformation of India. *Geophys. Res. Lett.* **28**, 647–650 (2001).

6. Bilham, R., Engdahl, R., Feldl, N. & Satyabala, S. P. Partial and complete rupture of the Indo-Andaman plate boundary 1847–2004. *Seismol. Res. Lett.* **76**, 299–311 (2005).

7. Newcomb, K. R. & McCann, W. R. Seismic history and seismotectonics of the Sunda Arc. *J. Geophys. Res.* **92**, 421–439 (1987).

8. Zachariasen, J., Sieh, K., Taylor, F. W. R., Edwards, R. L. & Hantoro, W. S. Submergence and uplift associated with the giant 1833 Sumatran subduction earthquake: Evidence from coral microatolls. *J. Geophys. Res.* **104**(B1), 895–920 (1999).

9. Sieh, K., Natawidjaja, D., Chlieh, M., Galetzka, J. & Avouac, J. P. The giant subduction earthquakes of 1797 and 1833, West Sumatra: Characteristic couplets, uncharacteristic slip. *Eos* **85** (Fall Meeting Suppl.), abstr. T12B–04 (2004).

10. Ni, S., Kanamori, H. & Helmberger, D. Energy radiation from the Sumatra earthquake. *Nature* **434**, 582 (2005).

11. Guilbert, J., Roueff, A., Vergoz, J. & Cansi, Y. An original image of the seismic rupture of the Sumatra M_w = 9.0 using PMCC from seismic and hydroacoustic small array. *Geophys. Res. Lett.* **32**, L15310, doi:10.1029/ 2005GL022966 (2005).

12. de Groot-Hedlin, C. D. Estimation of the rupture length and velocity of the Great Sumatra earthquake of Dec 26, 2004 using hydroacoustic signals. *Geophys. Res. Lett.* **32**, L11303, doi:10.1029/2005GLO22695 (2005).

13. Lay, T. *et al*. The great Sumatra–Andaman earthquake of 26 December 2004. *Science* **308**, 1127–1133 (2005).

14. Ammon, C. J. *et al*. Rupture process of the 2004 Sumatra–Andaman earthquake. *Science* **308**, 1133–1139 (2005).

15. Prawirodirdjo, L. *et al*. Geodetic observations of interseismic strain segmentation at the Sumatra subduction zone. *Geophys. Res. Lett.* **24**, 2601–2604 (1997).

16. McCaffrey, R. *et al*. Strain partitioning during oblique plate convergence in northern Sumatra: Geodetic and seismologic constraints and numerical modeling. *J. Geophys. Res.* **105**, 28363–28376 (2000).

17. Vigny, C. *et al*. Insight into the 2004 Sumatra–Andaman earthquake from GPS measurements in southeast Asia. *Nature* **436**, 201–206 (2005).

18. Nikolaidis, R. Observation of geodetic and seismic deformation with the Global Positioning System. PhD thesis, Univ. California, San Diego (2002).

19. Altamimi, Z., Sillard, P. & Boucher, C. ITRF2000: A new release of the International Terrestrial Reference frame for earth science applications. *J. Geophys. Res.* **107** (B10), 2214, doi:10.1029/2001JB000561 (2002).

20. Natawidjaja, D. H. *et al*. Paleogeodetic records of seismic and aseismic subduction from central Sumatran microatolls, Indonesia. *J. Geophys. Res.* **109**, doi:10.1029/2003JB0002398 (2004).

21. Zachariasen, J., Sieh, K., Taylor, F. W. & Hantoro, W. S. Modern vertical deformation above the Sumatran subduction zone: Paleogeodetic insights from coral microatolls. *Bull. Seismol. Soc. Am.* **90**, 897–913 (2000).

22. Agnew, D. C. NLOADF: a program for computing ocean-tide loading. *J. Geophys. Res.* **102**, 5109–5110 (1997).

23. Meltzner, A. J. *et al*. Uplift and subsidence associated with the great Aceh-Andaman earthquake of 2004. *J. Geophys. Res.* **111**, doi:10.1029/2005JB003891 (2006).

24. Jade, J., Ananda, M. B., Dileep Kumar, P. & Banerjee, S. Co-seismic and post-seismic displacements in Andaman and Nicobar Islands from GPS measurements. *Curr. Sci.* **88**, 1980–1984 (2005).

25. Ruff, L. & Kanamori, H. Seismicity and the subduction process. *Phys. Earth Planet. Inter.* **23**, 240–252 (1980).

26. Kanamori, H. in *Earthquakes: Observation, Theory and Interpretation* (eds Kanamori, H. & Bosch, E.) 597 (North Holland, New York, 1983).

27. Uyeda, S. & Kanamori, H. Back-arc opening and the model of subduction. *J. Geophys. Res.* **84**, 1049–1061 (1979).

28. Scholz, C. H. & Campos, J. On the mechanism of seismic decoupling and back-arc spreading at subduction zones. *J. Geophys. Res.* **100**, 22103–22115 (1995).

29. McCaffrey, R. Influences of recurrence times and fault zone temperatures on the age-rate dependence of subduction zone seismicity. *J. Geophys. Res.* **102**, 22839–22854 (1997).

30. Natawidjaja, D. H. *et al*. The giant Sumatran megathrust ruptures of 1797 and 1833: Paleoseismic evidence from coral microatolls. *J. Geophys. Res.* (in the press).

31. Chlieh, M., Avouac, J., Sieh, K., Natawidjaja, D. & Galetzka, J. Investigating lateral variations of interseismic strain along the Sumatran subduction zone. *Eos* **85** (Fall

Meeting Suppl.), abstr. T13C–1385 (2004).

32. McCaffrey, R. Crustal block rotations and plate coupling. In *Plate Boundary Zones* (eds Stein, S. & Freymueller, J.) 101–122, doi:10.1029/030GD06 (AGU Geodynamics Series 30, Washington DC, 2002).

33. Simoes, M., Avouac, J.-P., Cattin, R. & Henry, P. The Sumatra subduction zone: a case for a locked fault zone extending into the mantle. *J. Geophys. Res.* **109**, doi:10.1029/2003JB002958 (2004).

34. Bollinger, L., Avouac, J. P., Cattin, R. & Pandey, M. R. Stress buildup in the Himalaya. *J. Geophys. Res.* **109**, doi:10.129/2003JB002911 (2004).

35. Miyazaki, S., Segall, P., Fukuda, J. & Kato, T. Space time distribution of afterslip following the 2003 Tokachi-oki earthquake: Implications for variations in fault zone frictional properties. *Geophys. Res. Lett.* **31**, doi:10.1029/2003GL019410 (2004).

36. Cohen, S. C. On the rapid postseismic uplift along Turnagain Arm, Alaska following the 1964 Prince William Sound Earthquake. *Geophys. Res. Lett.* **25**, 1213–1215 (1998).

37. Hutton, W., DeMets, C., Sanchez, O., Suarez, G. & Stock, J. Slip kinematics and dynamics during and after the 1995 October 9 M-w = 8.0 Colima-Jalisco earthquake, Mexico, from GPS geodetic constraints. *Geophys. J. Int.* **146**, 637–658 (2001).

38. Hsu, Y. J. *et al*. Rapid afterslip following the 1999 Chi-Chi, Taiwan earthquake. *Geophys. Res. Lett.* **29**, doi:10.1029/2002GL014967 (2002).

39. Scholz, C. *The Mechanics of Earthquakes and Faulting* Ch. 2 (Cambridge Univ. Press, New York, 1990).

40. Hyndman, R. D., Yamano, M. & Oleskevich, D. A. The seismogenic zone of subduction thrust faults. *The Island Arc* **6**, 244–260 (1997).

41. Pacheco, J. F., Sykes, L. R. & Scholz, C. H. Nature of seismic coupling along simple

plate boundaries of the subduction type. *J. Geophys. Res.* **98**, 14133–14160 (1993).

42. Brune, J. N. Seismic moment, seismicity, and rate of slip along major fault zones. *J. Geophys. Res.* **73**, 777–784 (1968).

43. Curray, J. Tectonics and history of the Andaman Sea region. *J. Asian Earth Sci.* **25**, 187–232 (2005).

44. Engdhal, E., van der Hilst, R. & Buland, R. Global teleseismic earthquake relocation with improved travel times and procedures for depth determination. *Bull. Seismol. Soc. Amer.* **88**, 722–743 (1998).

45. Tsai, V. C., Nettles, M., Ekstrom, G. & Dziewonski, A. M. Multiple CMT source analysis of the 2004 Sumatra earthquake. *Geophys. Res. Lett.* **32**, L17304, doi:10.1029/2005GL023813 (2005).

List of Figures

Figure 1 **Tectonic setting and ruptures of major interplate earthquakes along the Sunda megathrust.** The yellow patches are estimated rupture areas of known large subduction events between 1797 and 2004 (refs 7, 9, 20). Orange patches depict the 2004 Sumatra–Andaman rupture where slip was 5 m or more. Tectonic features are simplified from Curray[43] and Natawidjaja *et al.*[20]. The boundary between Australia and India is a diffuse plate boundary between ~5° S and 8° N (ref. 44). Plate velocities of Australia (black arrows) and India (red arrows) relative to Sunda were computed from a regional kinematic model[1]. Dashed lines are contours of sediment thickness at intervals of 2,000 m. The inset shows that the age of the sea floor increases northwards, from ~50 Myr in the epicentral area to 80–120 Myr at the latitude of the Andaman islands.

Figure 2 **Comparison of near-field geodetic measurements (black arrows) with predictions (green arrows) of the seismic model III of ref. 14.** This comparison suggests that the geodetic data require more slip, a different spatial distribution of slip, or both. The inset shows a close-up of the Simeulue area. Horizontal displacements are shown with 95% confidence ellipses (see tables in Supplementary Information 1). Vectors in the Andaman and Nicobar islands are from CESS (http://www.seires.net/content/view/123/52/).

Figure 3 **Fault slip distribution determined from the geodetic data. a**, Model A. The distribution of combined coseismic and one-month post-seismic slip on the Sunda megathrust estimated from inversion of geodetic data shown in Fig. 2, including 30-day estimates of displacements from the permanent GPS stations at Medan (SAMP) and Phuket (PHKT)[17]. Black contour lines of slip are at 5-m intervals. Displacements computed from this model (green arrows for the horizontal and red arrows for the vertical at the sites used in the inversion, blue arrows at the other sites) are compared with the survey-mode

observations and with displacements over the first day estimated at continuous GPS stations in Thailand and Malayasia[17] (red arrows). Displacements are shown with 95% confidence ellipses. The comparison shows that significant postseismic displacements occurred in the first month following the rupture. The lower inset in **a** is a close-up view of predicted and measured vertical displacements on Simeulue Island. The upper inset in a shows a comparison of ruptured area (where slip exceeds 5 m in the model) with seismicity before the Sumatra–Andaman earthquake (1964–2002)[44]. 'Beach ball' symbols show local mechanisms determined from the geodetic model. Each focal mechanism corresponds to the summation of moment tensor within a 2° wide latitudinal bin. Slip vector azimuth of aftershocks (red lines) and foreshocks (black lines) are nearly parallel to slip azimuth during the main shock. **b**, Model B. The distribution of co- and post-seismic seismic slip on the Sunda megathrust estimated from inversion of geodetic data. Light contours of slip are at 5-m intervals starting at 5 m. Red vectors (with 95% confidence ellipses) are observed displacements and black are predicted. Coloured dots show locations of uplift constraints; those that are outlined were not fitted at the 2-σ level (hinge-line points were not used in this inversion). Small arrows near the Sunda trench show seismological estimates of coseismic slip directions in green[45] and geodetic estimates in grey. The insets show trench-normal profiles of earthquakes[44] (blue dots), megathrust (red curve), and slip amplitudes (purple curves). This model indicates up to 30 m of slip at depths of only 12–20km, northwest of nucleation and where the large Aceh tsunami originated.

Figure 4 **Latitudinal variations of scalar moments as determined from seismic waveforms (model III of ref. 14) and from geodetic data.** Moment released per half degree in latitude. Both geodetic models imply a rougher slip distribution than the seismic model. The total moment for geodetic model A (8.78×10^{22} Nm) exceeds the seismic moment by 30% ± 12%. This excess presumably reflects afterslip during the 30 days following the main shock.

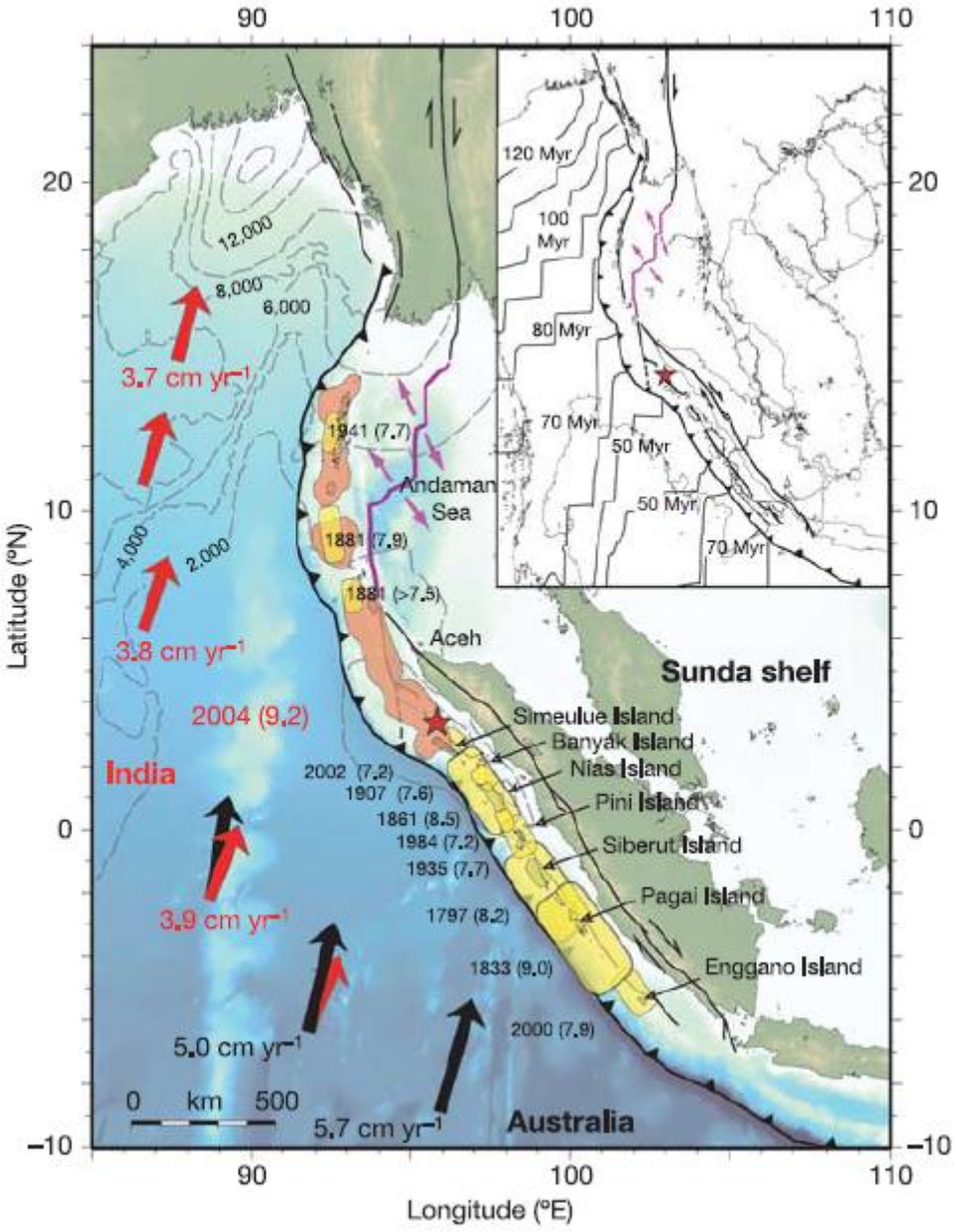
90
100
110
20
10
0
−10
Latitude (°N)
Longitude (°E)
120 Myr
100 Myr
80 Myr
70 Myr
50 Myr
50 Myr
70 Myr
12,000
8,000
6,000
4,000
2,000
3.7 cm yr⁻¹
3.8 cm yr⁻¹
3.9 cm yr⁻¹
5.0 cm yr⁻¹
5.7 cm yr⁻¹
1941 (7.7)
1881 (7.9)
1881 (>7.5)
Andaman Sea
Aceh
2004 (9.2)
India
Sunda shelf
Simeulue Island
Banyak Island
Nias Island
Pini Island
Siberut Island
Pagai Island
Enggano Island
2002 (7.2)
1907 (7.6)
1861 (8.5)
1984 (7.2)
1935 (7.7)
1797 (8.2)
1833 (9.0)
2000 (7.9)
0 km 500
Australia

Figure 1

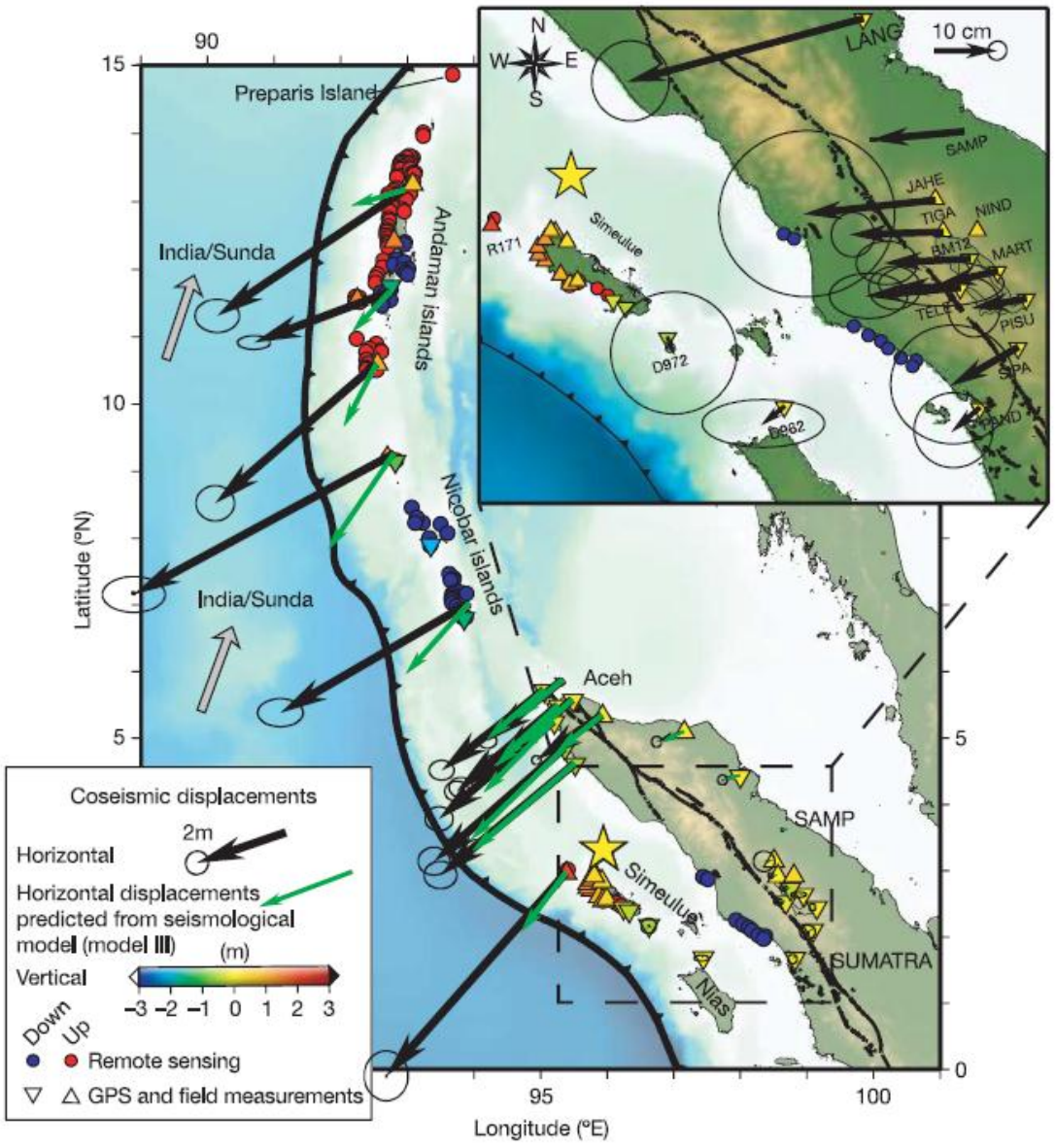
90
15
10
5
Latitude (°N)
Longitude (°E)
95
100
0
5
Preparis Island
India/Sunda
Andaman islands
Nicobar islands
India/Sunda
Aceh
SAMP
Simeulue
SUMATRA
Nias
N
W
E
S
10 cm
LANG
SAMP
JAHE
TIGA
NIND
BMTI2
MART
TELE
PISU
SIPA
PBAN
R171
Simeulue
D972
D962
Coseismic displacements
2m
Horizontal
Horizontal displacements predicted from seismological model (model III)
(m)
Vertical
−3 −2 −1 0 1 2 3
Down
Up
Remote sensing
GPS and field measurements

Figure 2

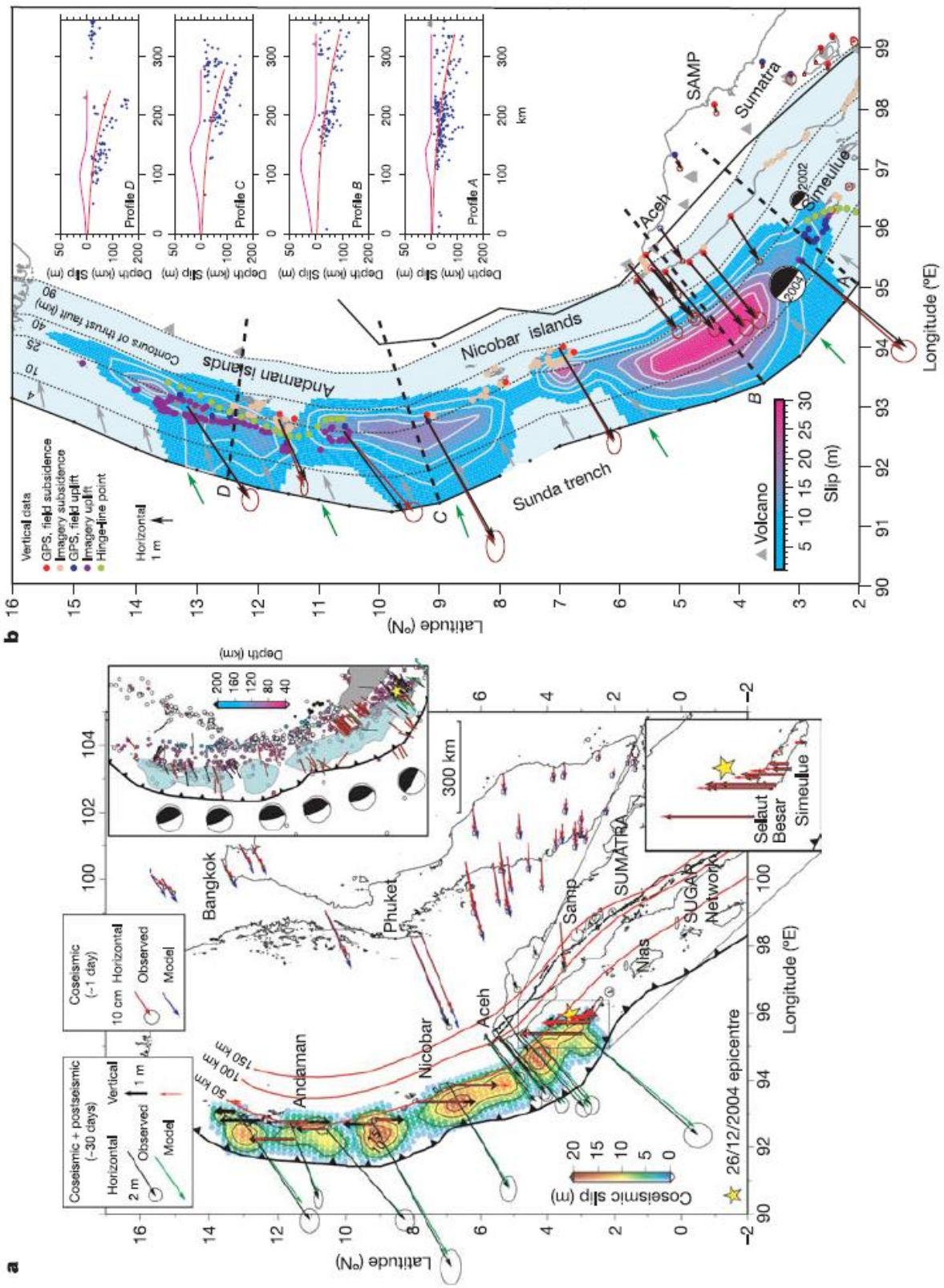
a
b
Coseismic + postseismic (~30 days)
Horizontal
Vertical
2 m
1 m
Observed
Model
Coseismic (~1 day)
10 cm Horizontal
Observed
Model
Coseismic slip (m)
20 15 10 5 0
26/12/2004 epicentre
Andaman
Nicobar
Aceh
Bangkok
Phuket
Samp
SUMATRA
SUGAR Network
Nias
Selaut Besar
Simeulue
300 km
50 km
100 km
150 km
Depth (km)
200 160 120 80 40
Latitude (°N)
Longitude (°E)
Vertical data
GPS, field subsidence
Imagery subsidence
GPS, field uplift
Imagery uplift
Hinge-line point
Horizontal
1 m
Andaman Islands
Contours of thrust fault (km)
Nicobar islands
Sunda trench
Volcano
Slip (m)
5 10 15 20 25 30
SAMP
Sumatra
Aceh
Simeulue
2002
2004
A
B
C
D
Profile D
Profile C
Profile B
Profile A
Depth (km) Slip (m)
km

Figure 3

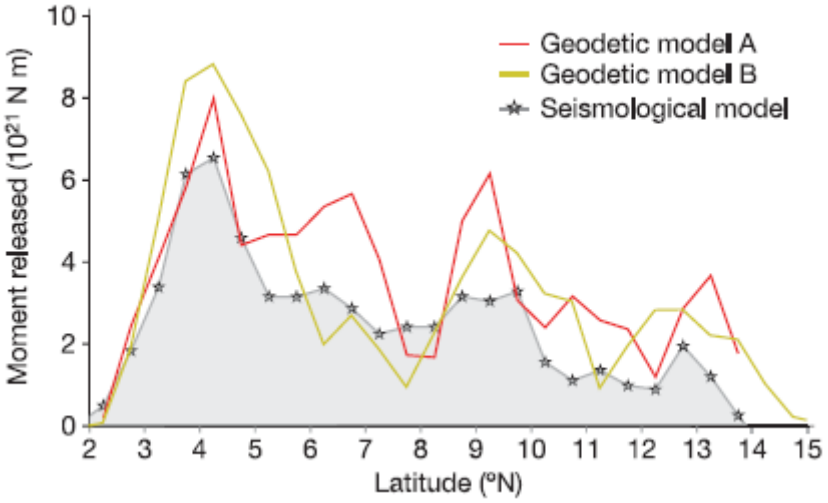
Geodetic model A
Geodetic model B
Seismological model
Moment released (10^{21} N m)
Latitude (ºN)
0
2
4
6
8
10
2
3
4
5
6
7
8
9
10
11
12
13
14
15

Figure 4